

CEREBROSPINAL FLUID FLOW BEHAVIOUR IN LUMBAR SPINAL STENOSIS – A COMPUTATIONAL FLUID DYNAMIC STUDY BASED ON MAGNETIC RESONANCE IMAGING

DR. TIE TECK LIANG

Dissertation Submitted For Partial Fulfilment of Master of
Medicine (Orthopaedic)



UNIVERSITI SAINS MALAYSIA

2018

ACKNOWLEDGEMENT

I would like to express my deepest gratitude to all directly and indirectly who had been involved and made this dissertation a reality. This work would not have been possible without all the support and encouragement. Special thanks to my supervisor, Associate Professor Dato Dr. Abdul Halim Yusof, Senior Consultant and Specialist of Orthopaedic Department of Hospital Universiti Sains Malaysia (Hospital USM) for his perseverance, guidance and constructive criticism throughout the process of producing this dissertation. Not forgetting, my co-supervisor, Associate Professor Dr. Kahar Bin Osman, Senior Consultant of Faculty of Bioscience and Medical Engineering, Universiti Teknologi Malaysia (UTM), and Dr. Ahmand Tarmizi Bin Musa, Lecturer and Radiologist of Hospital USM, who both guided me in the assessment of the study subjects.

Special thanks to Associate Professor Dr. Mohd Imran Yusof as the head of Orthopedic Department of Hospital USM for his support and encouragement.

Last but not least, a million thanks to my family members for their continuous support, encouragement and understanding and my greatest love to both my parents.

TABLE OF CONTENTS

	Page
Acknowledgement	i
Table of Contents	ii
List of Figures	v
List of Tables	viii
List of Abbreviations	xi
Abstrak	xii
Abstract	xiv
<u>Chapter 1: Introduction</u>	1
<u>Chapter 2: Literature Review</u>	
2.1 Epidemiology	3
2.2 Classification	6
2.3 Pathophysiology	10
2.4 Cerebrospinal Fluid (CSF)	14
2.4 Clinical Presentation of LSS	28
2.5 Imaging Technique	33
2.6 Treatment	43

Chapter 3: Hypothesis and Research Objectives

3.1	Research Objectives	47
3.2	Null Hypothesis	48

Chapter 4: Methodology

4.1	Study Design	49
4.2	Study Area	49
4.3	Source Population	49
4.4	Period of the Study	49
4.5	Inclusion Criteria for Study Group	50
4.6	Inclusion Criteria for Control Group	50
4.7	Exclusion Criteria	50
4.8	Calculation of Sample Size	51
4.9	Study Procedure	53
4.10	Flow Chart Statistical Analysis	58
4.11	Tested Variable	59
4.12	Statistical Analysis	60

Chapter 5: Results

5.1	Demographic	61
5.2	Characteristic of Mean Velocity	62
5.3	Characteristic of Mean Pressure in LSS	74
5.4	Characteristic of Mean WSS in LSS	76
5.5	Flow Pattern in LSS	77
5.6	Summary	81

Chapter 6: Discussion

6.1	Demographic Characteristics of The Patients	83
6.2	The Mean Velocity in LSS and Normal Spine	85
6.3	The Mean Pressure in LSS and Normal Spine	90
6.4	The Mean WSS with the Features of LSS	91
6.5	CSF Flow Pattern in LSS and Normal Spine	92

Chapter 7: Summary and Conclusion 93

Chapter 8: Limitation and Recommendation 94

LIST OF FIGURES

Figure 2.1 Prevalence of individuals with acquired LSS (%) according to the age groups.

Figure 2.2 Lumbar vertebrae. Potential regions of contact with nerve roots: 1 Central zone; 2 Entrance Zone; 3 Foramina (Mid) zone; 4 Extra-foramina (Exist) zone.

Figure 2.3 The degenerative cascade. The repetitive rotational strain or minor injury leads to the spectrum of degenerative changes causing degenerative and stenotic changes at the spine.

Figure 2.4 The diagram shows the flow patterns in a vascular bifurcation. At the straight region of arteries, the flow patterns are laminar (blue segments). At the branching region, some turbulent flows (red segments) are observed.

Figure 2.5 Diagram (a) shows an example of the qualitative prediction of CSF flow in the third ventricle and aqueduct of Sylvius in the healthy subject which allows the visual inspection of the flow in 3 dimension geometry. Diagram (b) is the examples of quantitative prediction of the velocity of the CSF flow in the healthy subject.

Figure 4.1 The 3D model image of the lumbar spine generated using MIMIC based on T2 weighted MRI images. The size of the spinal canal, spinal cord and the stenosis area are recreated based on the measurement.

Figure 4.2 The lateral view and the axial view of the 3D geometry created using SOLIDWORKS. The model consists of a smooth surface of the dura (A), the spinal canal that contains CSF spinal cord (B).

Figure 4.3 The coordination system is located in the centre of the spinal cord. This new coordination consists of 3 planes: x, y, and z.

Figure 4.4 The geometry meshes after identified the inlet, the outlet, and the wall using ANSYS FLUENT. Inflation is inserted. Nodes and elements are created after the geometry meshes.

- Figure 5.1 The mean velocity in different stenosis level based on the ROI.
- Figure 5.2 The mean velocity at the different disc level in relation to L4/L5 stenosis group and other stenosis group (L3/L4 & L4/L5 group, L4/L5 & L5/S1 group, and L3/L4, L4/L5 & L5/S1 group).
- Figure 5.3 The mean velocity in different degree of stenosis over the L3/L4 level at the ROI.
- Figure 5.4 The mean velocity in different degree of stenosis over the L4/L5 level at the ROI.
- Figure 5.5 The mean velocity in different degree of stenosis over the L5/S1 level at the ROI.
- Figure 5.6 The mean pressure in different stenosis level based on the ROI.
- Figure 5.7 The mean WSS in different stenosis level based on the ROI.

LIST OF TABLES

- Table 5.1 Demographic characteristics of all studied subjects.
- Table 5.2 Velocity magnitude contours along the L3/L4 level, L4/L5 level, and L5/S1 level for the healthy case.
- Table 5.3 Velocity magnitude contours along the L3/L4 level, L4/L5 level, and L5/S1 level for the mild degree of stenosis at the L4/L5 level.
- Table 5.4 Velocity magnitude contours along the L3/L4 level, L4/L5 level, and L5/S1 level for the moderate degree of stenosis at the L4/L5 level.
- Table 5.5 Velocity magnitude contours along the L3/L4 level, L4/L5 level, and L5/S1 level for the severe degree of stenosis at the L4/L5 level.
- Table 5.6 Velocity magnitude contours along the L3/L4 level, L4/L5 level, and L5/S1 level for stenosis at the L3/L4 level and L4/L5 level.

- Table 5.7 Velocity magnitude contours along the L3/L4 level, L4/L5 level, and L5/S1 level for stenosis at the L4/L5 level and L5/S1 level (above) and stenosis at the L3/L4, L4/L5 and L5/S1 level (below).
- Table 5.8 CSF flow patterns assessed virtually through streamline along the lumbar spine from L1/L2 level till L5/S1 level for normal subjects.
- Table 5.9 CSF flow patterns assessed virtually through streamline along the lumbar spine from L1/L2 level till L5/S1 level for mild degree of stenosis over the L4/L5 level.
- Table 5.10 CSF flow patterns assessed virtually through streamline along the lumbar spine from L1/L2 level till L5/S1 level for moderate degree of stenosis over the L4/L5 level.
- Table 5.11 CSF flow patterns assessed virtually through streamline along the lumbar spine from L1/L2 level till L5/S1 level for severe degree of stenosis over the L4/L5 level.
- Table 5.12 CSF flow patterns assessed virtually through streamline along the lumbar spine from L1/L2 level till L5/S1 level for L3/L4 and L4/L5 stenosis.

Table 5.13 CSF flow patterns assessed virtually through streamline along the lumbar spine from L1/L2 level till L5/S1 level for L4/L5 and L5/S1 stenosis.

Table 5.14 CSF flow patterns assessed virtually through streamline along the lumbar spine from L1/L2 level till L5/S1 level for L3/L4, L4/L5 and L5/S1 stenosis.

Table 5.15 Summary of the hydrodynamic parameters in different level of LSS according to the disc level in relation to the normal subjects.

LIST OF ABBREVIATIONS

LSS	Lumbar Spinal Stenosis
NC	Neurogenic Claudication
MRI	Magnetic Resonance Imaging
CSF	Cerebrospinal Fluid
CFD	Computational Fluid Dynamic
LBP	Low Back Pain
SG	Specific Gravity
WSS	Wall Shear Stress
Pa	Pascal
CT	Computed Tomography
3D	3 Dimensional
ROI	Region of Interest
Hospital USM	Hospital Universiti Sains Malaysia
M	Mean
SD	Standard Deviation

&

And

Abstrak

Pengenalan

Masalah penyempitan degeneratif tulang belakang (LSS) adalah patologi yang dicirikan oleh pemampatan unsur saraf dan struktur vaskular disebabkan oleh saluran tulang belakang lumbar yang sempit. Klinikal utama adalah claudication neurogenik. Patofisiologi tidak difahami sepenuhnya. Selalunya, manifestasi klinikal tidak sepadan dengan imej resonans magnetik (MRI).

Objektif

Tujuan kajian ini adalah untuk menentukan aliran cecair serebrospinal (CSF) dalam LSS degeneratif dengan menggunakan simulasi Permodelan Perkomputeraan Dinamik Bendalir (CFD) melalui ramalan aliran cecair kualitatif dan kuantitatif.

Kaedah

Kajian ini menilai 34 imej MRI terpilih, yang telah memenuhi kriteria inklusi dan pengecualian. T2 imej MRI digunakan untuk menilai tahap dan keterukan stenosis. Imej ini dipindahkan secara eletronik ke MIMIC dan SOLIDWORKS untuk generasi model dan

kemudian ke ANSYS FLUENT untuk simulasi CFD dengan keadaan sempadan yang telah ditetapkan. Akhirnya, hasil diesktrak mengikut kawasan kepentingan.

Keputusan

Halaju purata dalam kumpulan stenosis di peringkat L3/L4 dan L4/L5 adalah lebih rendah daripada kumpulan normal, tetapi ia lebih tinggi di peringkat L5/S1 untuk kumpulan stenosis. Kajian ini juga menunjukkan perbezaan yang tidak signifikan antara kumpulan stenosis dan kumpulan normal di peringkat L3/L4. Walau bagaimanapun, perbezaan yang signifikan dilaporkan pada peringkat L4/L5 ($p < 0.001$) dan L5/S1 ($p < 0.001$). Kajian ini menunjukkan keterukan stenosis tidak membawa pengaruh besar ke halaju CSF. Tekanan purata CSF dikurangkan dari peringkat L3/L4 ke peringkat L5/S1. Tekanan purata dalam kumpulan biasa adalah dari 981.47 Pa hingga 982.29 Pa, tetapi bagi kumpulan stenosis adalah dari 981.00 Pa hingga 983.00 Pa, bergantung kepada tahap stenosis. Purata tekanan geseran dinding (WSS) dalam kumpulan biasa adalah 0.019 Pa, dan kumpulan stenosis adalah 0.014 Pa hingga 0.024 Pa pada peringkat L3/L4. Tetapi, WSS tidak berbeza di peringkat L4/L5 (0.011 Pa) dan L5/S1 (0.007 Pa) untuk kedua-dua kumpulan biasa dan stenosis. Semua kumpulan menunjukkan corak aliran laminar dengan nombor Reynold dari 326.2 hingga 1312.57.

Rumusan

Halaju dalam LSS degeneratif tidak berbeza signifikan dalam kumpulan stenosis berbanding dengan kumpulan normal di peringkat L3/L4, namun kajian menunjukkan halaju berbeza signifikan untuk peringkat L4/L5 dan peringkat L5/S1. Tahap stenosis tidak mempengaruhi dengan merata pada kelajuan CSF. Tekanan berkurang apabila mengalir secara mendadak,

dan menunjukkan perbezaan yang tidak penting, Tidak berbeza signifikan ditunjukkan dalam WSS and corak aliran antara kumpulan normal dan kumpulan LSS degeneratif.

Abstract

Introduction

Degenerative lumbar spinal stenosis (LSS) is a pathology characterized by compression of neural elements and vascular structures due to a narrowed lumbar spinal canal. The main clinical presentation is neurogenic claudication. The pathophysiology is not entirely understood. Often, the clinical manifestation is not corresponding to the finding in magnetic resonance images (MRI).

Objective

The aim of this study is to determine the behaviour of cerebrospinal fluid (CSF) flow in degenerative LSS by using computational fluid dynamic (CFD) simulation through the qualitative and quantitative prediction of fluid flow and comparing with the flow in the normal spine.

Methods

This cross-sectional study evaluated the selected 34 MRI images, which had fulfilled the inclusion and exclusion criteria. The T2 weighted MRI images were used to assess the level and degree of stenosis. These images were transferred electronically to MIMIC and

SOLIDWORKS for model generation and then to ANSYS FLUENT for the CFD simulations with the predetermined boundary condition. Lastly, the results were extracted according to the region of interest (ROI).

Results

The mean velocity in stenosis groups at L3/L4 disc level and L4/L5 disc level was relatively lower than the normal group, but it was higher at the L5/S1 disc level for the stenosis groups. This study revealed an insignificant difference between the normal groups and the stenosis groups at L3/L4 disc level. However, significant differences between the stenosis group and the normal group at L4/L5 disc level ($p < 0.001$) and L5/S1 disc level ($p < 0.001$) were reported. This study demonstrated the severity of stenosis did not carry a great influence toward the CSF velocity. The mean pressure of the CSF reduced from L3/L4 disc level to L5/S1 disc level. The mean pressure in the normal group was ranging from 981.47 Pa to 982.29 Pa, but for stenosis group was ranging from 981.00 Pa to 983.00 Pa, depending on the stenosis level. The mean wall shear stress (WSS) in normal group was 0.019 Pa, and stenosis group was ranging 0.014 Pa to 0.024 Pa at L3/L4 disc level. However, indifferent mean WSS was showed at the L4/L5, and L5/S1 disc level revealed the (0.011 Pa and 0.007 Pa, respectively) for both normal and stenosis groups. All the streamlines demonstrated a laminar flow pattern regardless the normal spine or stenotic spine with their Reynold's number ranging from 326.2 to 1312.57.

Conclusion

The mean velocity in degenerative LSS did not differ significantly in stenosis group compared to the normal group at L3/L4 disc level, but the study showed the mean velocity

differ significantly for L4/L5 disc level and L5/S1 disc level. The degree of stenosis did not influence significantly on the mean velocity. The mean pressure reduced when flowed caudally, and showed insignificant different. Insignificant different was showed in the mean WSS as well as the flow pattern between the normal groups and degenerative LSS groups.

Chapter 1: Introduction

Lumbar spinal stenosis (LSS) is chronic pathology which is characterized by reducing either anteroposterior or transverse diameter of the lumbar spinal canal, nerve root canal or secondary to soft tissue, bone or both compression (Devlin, 2012a). Typically, the patients complain of either neurogenic claudication (NC) or radicular pain to lower extremities.

However, the pathophysiology of LSS is still not fully understood. Many patients even with severe stenosis may present with a minimal clinical sign and vice versa. The widely accepted explanations regarding the reason on clinical manifestation are the disturbance of blood supply and mechanical compression to the neural component (Genevay and Atlas, 2010). The magnetic resonance imaging (MRI), an imaging modality using radiofrequency pulses on the tissues in a magnetic field (Akay *et al.*, 2015), has gained its popularity in helping to diagnose LSS and determine the underlying pathology in LSS.

However, there are many cases where the MRI images and clinical manifestations are not corresponding to each other (Amundsen *et al.*, 1995). For example, in some cases where the MRI images show compression of the nerve roots at L3/L4, L4/L5, and L5/S1. However, the clinical symptoms present as only L5 nerve roots compression. By just doing decompression at the L4/L5 level, the clinical symptoms usually resolved without the need to decompress either L3/L4 or L5/S1 level. These are unable to be explained by the theories mentioned above. Thus, it raises the interest on other possible causes that may contribute to the pathophysiology of LSS.

The characteristic of cerebrospinal fluid (CSF) flow becomes one of the interest fields in understanding as a possible cause of LSS manifestation. With the help of MRI, examination of CSF flow pattern is possible. The CSF flow has been widely examined in the different central nervous system related pathologies, especially hydrocephalus and Chiari 1 malformation. Nevertheless, the information regarding dynamic of CSF flow and its importance in spinal stenosis is still insufficient.

Although MRI has been widely used to study the CSF flow, the computational fluid dynamic (CFD), an in vitro method can be used to investigate the qualitative and quantitative prediction of the CSF flow (Ferziger and Peric, 2002). By using the CFD method to study the CSF flow which includes the velocity of the flow, the flow pattern, pressure distribution and also wall shear stress, is possible.

Chapter 2: Literature Reviews

2.1 Epidemiology

Lumbar spinal stenosis (LSS) is a benign pathology which characterized by narrowing of the lumbar spinal canal, nerve root canal or intervertebral space (Devlin, 2012a). The reduction of the canal size can be due to the bony component, soft tissue component, or both. This osteo-ligamentous structures cause the compression of the neural elements, vascular structure and also disturb the fluid flow in the canal (Postacchini, 1995).

The actual prevalence of degenerative LSS is not well known. The prevalence is different in varies studies. It ranges from 1.7% to 13.1% (Kalichman *et al.*, 2009). The prevalence is increasing continuously due to the aging. This prevalence is evidenced by one of the most common reasons for the clinic visit and spinal operation in the aging population. (Deasy, 2015). The similar finding reported by other studies, where the prevalence increases dramatically in the population more than 50 years old irrespective of the gender (Issack *et al.*, 2012; Kalichman *et al.*, 2009; Yabuki *et al.*, 2013). Figure 2.1 demonstrates the relation between LSS prevalence and age group.

Often, the radiological findings are incidental. The prevalence of asymptomatic degenerative is hard to estimate. The Wakayama Spine Study reported 77.9% of the asymptomatic population might have moderate stenosis while 13.1% of the population with severe stenosis (Ishimoto *et al.*, 2013). This finding is corresponding to other studies which stated that the relationship between radiographic imaging and clinical manifestation of the LSS is not well clarified (Amundsen *et al.*, 1995; Boden *et al.*, 1990; Ishimoto *et al.*, 2013).

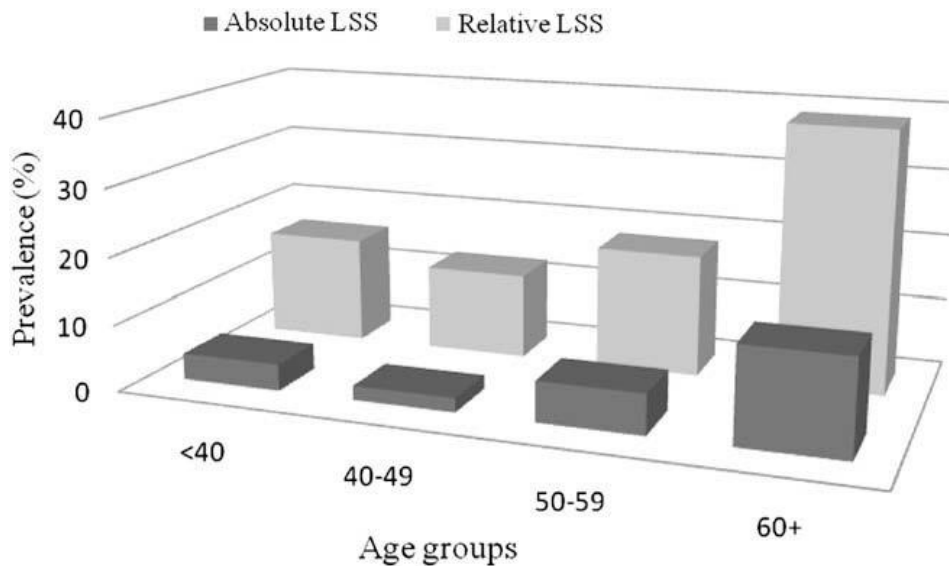


Figure 2.1: Prevalence of individuals with acquired LSS (%) according to the age groups (Kalichman *et al.*, 2009).

Symptomatic LSS often refers to patients present with NC or radicular pain with positive radiographic imaging is reported as 17.5% (Ishimoto *et al.*, 2013). Patients usually give a history of tiredness, clamping, paraesthesia at lower limb that is relieved by a short rest. However, present of clinical symptoms does not always equal to LSS. For example, some patients with peripheral artery disease can have symptoms like NC in the absence of LSS.

In Malaysia, the prevalence of LSS is not well established. The only report on the incidence of low back pain (LBP) is available. The prevalence LBP is about 12 % in semi-rural population and 60% of the population at risk (Hussein *et al.*). A similar result was reported with cumulative life prevalence of LBP as 72.5% (Wong *et al.*, 2010).

Based on clinical observation, the majority of the stenosis occurs at L4/L5 level. This finding is parallel with the reported prevalence for L4/L5 level as 93%, with 66% for L3/L4 level and the L5/S1 level is 49% (Tomkins-Lane *et al.*, 2014). However, this prevalence is only applicable for central stenosis due to higher mobility and rotational movement at the L4/L5 level and L3/L4 level. At the meantime, the L5/S1 level locates below the intracrestal line, with strong ligaments attaching to the transverse processes and has a larger canal. These features explain the lower incidence at L5/S1 level. As for the lateral stenosis, the affected level will be L4/L5 followed by L5/S1. This phenomenon suggests the protective mechanism may not apply in lateral stenosis.

2.2 Classification

2.2.1 Etiologic Classification

Two main types of LSS are being described based on etiology. They are congenital developmental stenosis and acquired stenosis (Devlin, 2012a). This type of stenosis is characterized by the narrowed canal size secondary to the anatomical variation and leading to the multilevel neural elements compression that presents at earlier in age with less degenerative changes (Singh *et al.*, 2005). This form of stenosis consists of idiopathic spinal stenosis, achondroplastic, spinal dysraphism, failure of vertebral segmentation, Morquio-Ulrich syndrome (Devlin, 2012a; Fritz *et al.*, 1998).

Secondary or acquired LSS is more common in the clinical presentation than primary stenosis. It is common in the aging population with multiple degenerative changes over the musculoskeletal. Degenerative, spondylolisthetic, iatrogenic (secondary to laminectomy or spinal fusion), post-traumatic, metabolic (Paget's disease, Fluorosis), osteoporotic fracture, spinal metastasis and combined form are the variants of acquired LSS (Devlin, 2012a).

2.2.2 Anatomic Classification

The etiologic classification only provides the information regarding the possible underlying cause of LSS. It does not give the detail regarding pathology site, explains the differences in clinical manifestation and provides the strategies of management.

Based on the anatomical site of narrowing, the LSS is divided into the central stenosis and lateral stenosis (An and Glover, 1994; Szpalski and Gunzburg, 2003; Verbiest, 1954). Reducing the anterior-posterior diameter of the central canal is known as central stenosis. It is due to the intervertebral disc degeneration and reduces its height, the facet joint or ligamentum flavum hypertrophy (Devlin, 2012a; Szpalski and Gunzburg, 2003).

Different terminologies such as lateral recess stenosis, subarticular stenosis, intervertebral foramina stenosis used to describe the lateral stenosis. These terms lead to confusion when communication among the clinician. To overcome the problem, the scientists divide lateral stenosis into three zones, namely the entrance zone, foramina zone and extra-foramina zone (Lee *et al.*, 1988).

The entrance zone is medial to the superior articular process. At this zone, it contains nerve root and dura which bathed in CSF. Osteophyte over the superior articular process, superior margin of the lamina, hypertrophy of the facet joints, short pedicle may cause stenosis in this zone.

The foramina zone is also known as mid zone. It is bounded by pars interarticularis with part of the lamina, below the pedicle. Medially, it opens to central canal. It contains dorsal root ganglion, ventral motor nerve, dura, and CSF. The leading causes of stenosis at this zone are osteophyte over the pars interarticularis and either fibrocartilaginous or bursal tissue hypertrophy.

The intervertebral foramen, lateral aspect of the facet joint and disc which is one level below the entrance zone forms the extra-foraminal (exit) zone. This region contains peripheral nerves. The pathologies can be due to hypertrophy or osteoarthritic changes of the facet joint and the osteophyte over the foramen.

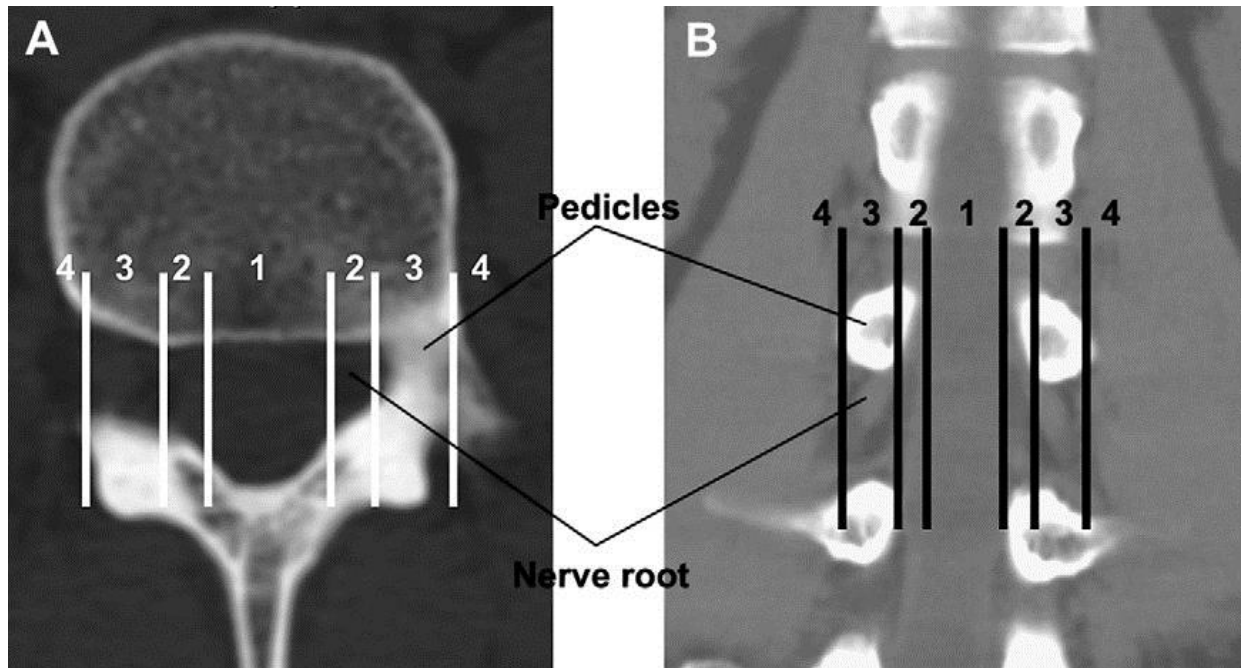


Figure 2.2: Lumbar vertebrae. Potential regions of contact with nerve roots: 1 Central zone; 2 Entrance Zone; 3 Foramina (Mid) zone; 4 Extra-foramina (Exist) zone (Jenis and An, 2000).

2.2.3 According to the Degree of Stenosis

With the mentioned classifications are still unable to explain the reason of asymptomatic presentation in LSS. Thus, using the anteroposterior diameter of the canal to describe the degree of stenosis gains its popularity. The diameter ranges from 10 mm to 12 mm considers as “relative stenosis” and less than 10 mm as “absolute stenosis” (Verbiest, 1954). This description is still widely used until today because it is easier to measure.

The sagittal diameter of the spinal canal subsequently is measured and categorized the stenosis into the normal spine, moderate stenosis and severe stenosis with the diameter more 10 mm, 8 mm to 10 mm and less than 8 mm, respectively (Kalichman *et al.*, 2009). However, this classification does not categorize the mild degree of stenosis.

Different studies have been trying to classify the stenosis by establishing the relationship between the quantitative parameter with patient's disability. One of the methods is the measurement of the cross-sectional area of the dural sac. The cross-sectional area of more than 130 mm² consider as the normal lumbar spine, 100 mm² till 129 mm² as mild canal stenosis, with the cross-sectional area of 75 mm² till 99 mm² define the moderate stenosis and less than 75 mm² as severe stenosis. (Hughes *et al.*, 2015; Schonstrom *et al.*, 1985)

Other parameters include the stenotic index (Schizas *et al.*, 2010), features of cauda equina on MRI (Guen *et al.*, 2011), the interpedicular distance and lateral recess angle (Hughes *et al.*, 2015) reported in various journal trying to classify the LSS. However, they are less popular because these classifications provide a neither good inter-observer nor intra-observer reliability. Moreover, they are technically more challenging in measurement. Thus, until today, none of the classification is considered well established to explain the relationship between radiological findings with the clinical symptoms.

2.3 Pathophysiology

Aging is the only well-established risk factor for degenerative LSS. Other factors, such as mechanical, biochemical, traumatic, nutrition, congenital deformity and genetic may contribute to the degenerative process (Devlin, 2012b). However, their importance is still not well understood.

Recently, several studies reported the prevalence of LSS in the diabetic patients is 28%, which suggestive of a strong connection between diabetes mellitus with degenerative LSS (Anekstein *et al.*, 2010; Asadian *et al.*, 2016). Other than that, obesity and overweight also reported as a risk factor for degenerative LSS. The incidence rate ratio is 1.68 (95% CI, 1.54-1.83) for the overweight group and 2.18 (95% CI, 1.87-2.53) for the obese population (Knutsson *et al.*, 2015). However, the socioeconomic profile has not proven as a significant risk factor for degenerative LSS, but it contributes to LBP incidence (Katz, 2006; Wong *et al.*, 2010).

According to the degeneration cascade of the spine, the progression is divided into three phase: dysfunction, instability, and stabilization (Devlin, 2012b; Kirkaldy-Willis *et al.*, 1978). The intervertebral disc and two zygapophyseal joints form the three-joint complex. This compound is known as a functional spine unit. Recurrent rotational strain or minor compression injury to one of the components of the complex will lead to injury to other parts. Subsequently, this will lead to the degenerative process in the spine (Kirkaldy-Willis *et al.*, 1978).

During the dysfunction phase, the injury causes a circumferential tear of annulus fibrosus and degeneration of the disc. The disc materials may herniate into the spinal canal. At the same time, synovitis, hypomobility and cartilage destruction occur at the facet joints. Followed by instability phase, which is characterized by capsular laxity, internal disc disruption and reduce disc height resulting joints subluxation and disc resorption. Thus, the lateral nerve entrapment may occur. At the stabilization phase, osteophytes formation over the disc and joints, enlargement of the articular process cause single level stenosis. Further rotational strain or compression injury at the levels above and below will cause multilevel spinal stenosis.

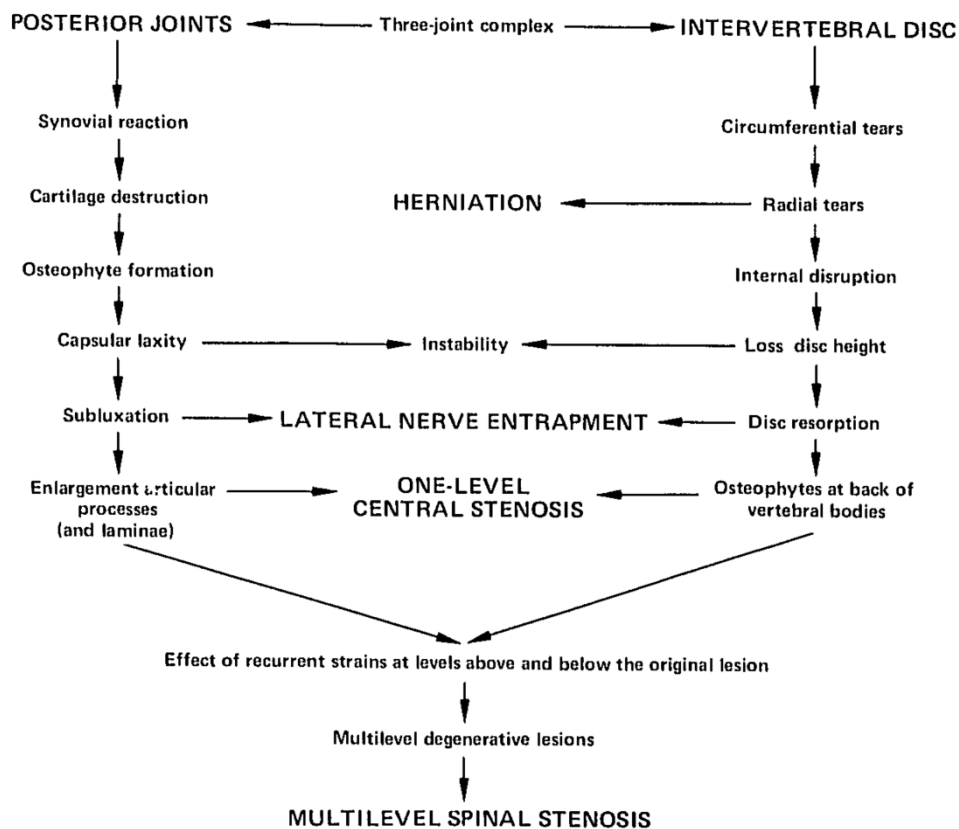


Figure 2.3: The degenerative cascade. The repetitive rotational strain or minor injury leads to the spectrum of degenerative changes causing degenerative and stenotic changes at the spine (Kirkaldy-Willis et al., 1978).

The osteophytes and herniated disc cause mechanical compression on the neural elements and vessels at the regions. These structures result in direct nerves compression, inflammation of the neural elements and surrounding tissues, the blood flow disturbance, microvascular changes, decreased nutritional supply, accumulation of harmful substances, oedema and fibrosis (Genevay and Atlas, 2010; Zingg and Boos, 2008).

The inflammatory process occurs at the nerve, synovial joints and a herniated disc is the primary cause of pain and reduces in nerve functions (Kobayashi *et al.*, 2005). This phenomenon is evidenced by increased inflammatory cytokine, the interleukin 1 in the degenerative LSS (Igarashi *et al.*, 2007) and the effectiveness of steroid injection at the facet joints or epidural space leading to a pain-free period (Davis *et al.*, 2016). Despite the positive result, some studies have shown the opposite (Friedly *et al.*, 2014).

Either arterial insufficiency or venous pooling may cause the neural component ischemia (Genevay and Atlas, 2010; Porter, 1996; Porter, 2000). The chemical mediators released from the Wallerian degeneration region may be one of the reasons in causing pain (Kobayashi, 2014). This theory is evidenced by the improvement of pain symptoms by using vasodilator, Prostaglandin E1 derivatives (Matsudaira *et al.*, 2009). However, it is not convincing enough for the vascular mechanism due to lack of data to support. Furthermore, the arterial insufficiency also results in reduce nutritional supply (Zingg and Boos, 2008).

These theories are still unable to explain the not correspondent finding between the clinical manifestation and the radiological images. Thus, it raises the interest of the hydrodynamic features of the CSF in a normal lumbar spinal canal and stenotic spine, whether an abnormal CSF flow in the stenotic spine can contribute to the clinical manifestations in LSS. Some of the clinical features of LSS are dynamic, such as the clinical symptoms are resolved by forwarding bending of the body and the occurrence of the NC after prolonged ambulation, also suggest the possibility of involvement of the CSF dynamics (Chun *et al.*, 2016).

2.4 Cerebrospinal Fluid

The lumbar spinal cord continues as conus medullaris which end at the L1/L2 level and subsequently becomes nerve roots that are bathed by CSF. CSF is an extracellular fluid in the nervous system. It is a clear colourless fluid surrounds the brain and spinal cord, and it circulates in the ventricular systems of the brain and subarachnoid space in the spinal cord (Agamanolis, 2013; Constanzo, 2010).

It maintains the optimum environment and homeostatic condition between the blood and the interstitial fluid for the neuron, drains the leaked protein and acts as a cushion around the brain and spinal cord (Bijlani and Manjunatha, 2011a). It also functions as cerebral autoregulation of the cerebral blood flow and immunological protection (Agamanolis, 2013; Constanzo, 2010). Whether these protective mechanisms will be altered in degenerative LSS secondary to the disturbed of CSF dynamic is yet established.

Through diffusion, pinocytosis, and active transfer mechanism, 95% of the fluid is produced from arterial blood by the epithelial cells of the choroid plexus at the lateral ventricles (Agamanolis, 2013; Greenberg, 2010). The ependymal cells of the ventricles and dura of the nerve root also produce a little amount of CSF (Agamanolis, 2013; Bijlani and Manjunatha, 2011a; Greenberg, 2010). The rate of formation is about 450 ml/day and regularly replaced three times a day. The reabsorption of CSF occurs in arachnoid villi at the subdural venous sinuses, lymphatic system, and choroid plexuses. The driving force of this absorption is the colloid osmotic pressure (Bijlani and Manjunatha, 2011a).

CSF is an extracellular fluid with pH of 7.33 to 7.35, specific gravity (SG) of 1.005 to 1.007 and pCO₂ of 47mmHg (Greenberg, 2010). The osmolarity of the fluid is 295 mOsm/l with 99% of water, 138 mEq/l of sodium, 2.8 mEq/l of potassium, 119 mEq/l of chloride, 2.1 mEq/l of calcium, 30 mg/dl of protein and 40-80 mg/dl of glucose (Greenberg, 2010).

2.4.1 Density of Cerebrospinal Fluid

The density of CSF is the degree of compactness of the CSF, with formula as mass/volume. While, the SG of CSF is the ratio of the density of the CSF to the density of water in the same volume, same temperature, and same pressure.

$$SG \text{ of CSF} = \frac{\text{density of CSF}}{\text{density of water}}$$

$$1.005 = \frac{\text{density of CSF}}{1000 \text{ kg/m}^3}$$

$$\text{Density of CSF} = 1005 \text{ kg/m}^3$$

where the density of water is 1000 kg/m³, and SG of CSF is 1.005.

Thus, the calculated density is range from 1005 kg/m³ to 1007 kg/m³. This finding is similar to few reported studies ranging from 1005 kg/m³ to 1007.5 kg/m³ (Hadzri *et al.*, 2011; Levin *et al.*, 1981).

However, the mean density of CSF in vivo at normal body temperature is $1000.5 \pm 0.2 \text{ kg/m}^3$ (Linninger *et al.*, 2009; Lui *et al.*, 1998; Schiffer *et al.*, 1999). This difference of the density might be due to the effect of body temperature. This finding is similar to the conclusion by Richardson and Wissler, where the mass, volume, and the temperature can significantly influence the accuracy of the density (Richardson and Wissler, 1996). Different subpopulations also have the slightly different density. The density in men is slightly higher than women, while density for premenopausal women, pregnant women, and postmenopausal women are also showing slight differences (Lui *et al.*, 1998; Masuda and Yokoyama, 1995; Schiffer *et al.*, 2002).

2.4.2 Viscosity

The measurement of the fluid resistance to deformation under stress influence is known as viscosity (Viswanath *et al.*, 2007). When the fluid displays as a linear relationship between the viscosity and shear stress, and the viscosity remain constant despite the stress applied the fluid is known as Newtonian fluid (Franco and Partal). CSF is a Newtonian fluid with its viscosity is 0.001 kg/(m-s) (Howden *et al.*, 2008; Linninger *et al.*, 2009). Thus, it has the similar viscosity as water. Although CSF contains a small amount of protein, glucose, and the electrolyte which may alter the viscosity, the study has shown that these solutes in CSF do not contribute a significant change in the viscosity (Bloomfield *et al.*, 1998).

2.4.3 Velocity

CSF continuously flows from the lateral ventricle toward the third ventricle then the fourth ventricle and leaving to subarachnoid space through foramina of Magendie and Luschka. Subsequently, the CSF flows caudally to the spinal cord at the subarachnoid space. The distance that CSF flows per units of time defines the velocity.

Study of the CSF velocity is possible by using phase contrast MRI or CINE phase contrast MRI. Several studies reported a broad range of normal mean velocity at the ventricles, ranging from 0.37 ± 0.18 cm/s (Akay *et al.*, 2015; Linninger *et al.*, 2009), 0.93 cm/s (Bhadelia *et al.*, 1995), 2.15 cm/s (Nitz *et al.*, 1992), 2.94 ± 0.94 cm/s (Kim *et al.*, 1999) till 9.99 ± 2.77 cm/s (Hasiloglu *et al.*, 2012). The velocity may be influenced by the parameter, gradient strength and technique used during the investigation (Yousef *et al.*, 2016).

At the foramen magnum, the normal velocity of CSF is ranging from 3.7 ± 1.2 cm/s to 5.6 ± 2.2 cm/s (Pahlavian *et al.*, 2014). The finding is similar to other studies, where the reported velocity is 3.6 ± 2.0 cm/s (Bunck *et al.*, 2011) and 5.2 ± 1.8 cm/s (Yiallourou *et al.*, 2012).

The velocity is 8.2 ± 2.4 cm/s at the cervical level (Bunck *et al.*, 2011). However, this finding is different from another study. Freund *et al* reported the mean velocity at the cervical region as 0.95 cm/s with the velocity continuously increase at the thoracic level until 4.7cm/s and then decrease to 0.96 cm/s at lumbar region (Freund *et al.*, 2001). A similar result at lumbar level is reported, ranging from 0.58 ± 0.23 cm/s to 1.07 ± 0.49 cm/s when patient at rest and 0.9 ± 0.33 cm/s to 1.35 ± 0.52 cm/s after patient walking (Chun *et al.*, 2016). The lowest velocity is noticed at sacral region, 0.16 ± 0.15 cm/s to 0.32 ± 0.33 cm/s (Chun *et al.*, 2016). However, these studies used a small sample size to investigate the velocity.

Mathematically, the velocity can be calculated using this equation: $v = \frac{Q}{A}$, where Q is the fluid flow, and A is the total cross-sectional areas of the fluid flow through (Bijlani and Manjunatha, 2011b). By assuming the CSF flow is constant, the CSF velocity is inversely proportionate to the total cross-sectional areas that parallel to the CSF flow. Thus, the velocity will increase in a reduced total cross section area.

This finding is further proven by the other studies, where the mean velocity is higher in the patient with Chiari 1 malformation, cervical stenosis, and lumbar stenosis. In Chiari 1 malformation, the reported mean velocities at foramen magnum are 5.8 ± 0.4 cm/s to 7.6 ± 0.8 cm/s (Pahlavian *et al.*, 2014), 10.9 cm/s (Bunck *et al.*, 2011), 11.8 ± 9 cm/s (Yiallourou *et al.*, 2012). This velocity increased to 19.5 cm/s in Chiari 1 malformation with syringomyelia (Bunck *et al.*, 2011).

Parkkola *et al* reported the velocity of CSF at the C2 in a mild cervical stenosis is ranging from 0.84 cm/s to 2.99 cm/s, 1.96 cm/s to 2.18 cm/s in moderate stenosis and 1.16 cm/s to 1.91 cm/s in severe stenosis (Parkkola *et al.*, 2000). Moreover, they concluded that this velocity is not affected by the degree of stenosis (Parkkola *et al.*, 2000). However, a higher velocity at C6 level is reported for C5/C6 and C6/C7 stenosis, 11.2 cm/s to 14.5 cm/s (Bunck *et al.*, 2011). This difference is due to the level used for velocity measurement. The former study measured the velocity at the C2 level despite the level of stenosis, while the latter study measured at the level of stenosis.

In the study performed by Chun *et al* regarding the flow velocity in patients with LSS, by measuring the velocity at the L2 level and S1 level at rest, and reported as 0.65 ± 0.22 cm/s and 0.11 ± 0.05 cm/s, respectively, but the velocity of CSF after the patient walking until the NC reproduce as 0.45 ± 0.19 cm/s to 0.66 ± 0.37 cm/s (Chun *et al.*, 2016). They concluded that the velocity does not affect by stenosis, but the reduction of velocity is significant in the patient with LSS after the symptoms are reproduced (Chun *et al.*, 2016). However, this study does not mention the level, degree, and the anatomical site of the stenosis.

2.4.4 Flow Pattern

Laminar flow and turbulent flow are two widely used terms in fluid dynamics. When the fluid flows in parallel layers with a well-ordered pattern it is known as laminar flow, while a dispersed flow is termed as turbulent (Janna, 2010). In medicine, these flow patterns are used to describe the flow in the blood vessels or the airway. The blood flows through the vessels in a laminar pattern, but a mild turbulent flow is observed at the branching site or in the pathological vessels. The similar phenomena observed in the respiratory system.

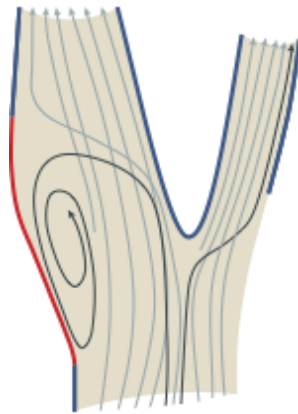


Figure 2.4: The diagram shows the flow patterns in a vascular bifurcation. At the straight region of arteries, the flow patterns are laminar (blue segments). At the branching region, some turbulent flows (red segments) are observed (Hahn and Schwartz, 2009).

The Reynold's number is used to determine the flow pattern, with *Reynold's number* = $\frac{SDV}{\eta}$, with D is the diameter of the tube, S is the density of the fluid, V is the velocity and η is the viscosity of the fluid (Bijlani and Manjunatha, 2011b). When the number is less than 2000, a laminar flow is observed. The flow is considered as turbulent with the value more than 3000. The transitional flow is termed when the number is between 2000 and 3000.

Based on the equation, the diameter of the structure, viscosity of the fluid as well as the velocity can influence Reynold's number. Theoretically, either larger diameter, higher velocity or reduce in viscosity are likely to cause turbulent flow. However, blood flow in a larger artery remains as a laminar pattern. The following equation explains this phenomenon:

$$diameter = \sqrt{\frac{4 \times flow\ rate}{\pi \times velocity}}$$

$$velocity = \frac{4 \times flow\ rate}{\pi \times diameter^2}$$

Therefore, the mean velocity of the flow is inverse to diameter squared (Klabunde, 2007). Thus, when the velocity decreases to one-fourth of its value when the diameter is doubled, and resulting in Reynold's number decreases by half.

The CSF flow pattern is often described as a periodic pattern under the cardiac output influence. During the systolic phase, the CSF flows caudally from foramen magnum and in a reverse direction during the diastolic phase (Iliff *et al.*, 2013). However, it is still believed that the flow is still a laminar pattern with the influence of cardiac output when it flows in subarachnoid space of the spinal cord (Jacobson *et al.*, 1996). By following the mentioned equation, a turbulent flow will be observed at the stenotic area. This flow pattern is because of the velocity will increase when the cross-sectional area of the canal is reduced secondary to the stenosis, and increasing Reynold's number.

2.4.5 Pressure

The ventricles and the subarachnoid space of the spinal cord together form a closed conduit. When this conduit filled with CSF, it generates pressure. Pressure is defined as the external force acting on a given surface area, $Pressure = \frac{Force}{Area}$, (Miller *et al.*, 2012). If the pressure remains same throughout the closed conduit, the fluid will be static.

According to the physical principle that applied to describe the blood flow, the blood flow in the vessel follows the Poiseuille's equation:

$$Q = (P1 - P2) \times \frac{\pi r^4}{8\eta l}$$

where Q is the flow rate, $(P_1 - P_2)$ is the pressure difference across the vessels, r is the radius of the vessels, η is the blood viscosity and l is the length of the vessels (Bijlani and Manjunatha, 2011b). This equation shows the pressure gradient in the vessels plays a significant role in blood flow. The blood only will flow in the vessels if the proximal pressure (P_1) is higher than the distal pressure (P_2).

The CSF pressure is also known as intracranial pressure (Bijlani and Manjunatha, 2011a). Study of the CSF pressure is possible by using the open pressure during the lumbar puncture, intraventricular catheter, intraparenchymal probe, subarachnoid probe, epidural probe, tympanic membrane displacement and transcranial doppler. The normal CSF pressure is 933.257 pascal (Pa) to 1999.835 Pa (7 mmHg to 15mmHg) (Steiner and Andrews, 2006). In a normal person, the pressure may differ by 133.322 Pa (1 mmHg) due to production and absorption of the CSF. This pressure gradient allows CSF to flow.

Bernoulli's principle explains the pressure changes when the fluid flows through a narrowed tube. With the increment of the fluid velocity when it passes through the narrowed tube, the pressure of the fluid will drop (Heil and Hazel, 2011). The velocity equation and Bernoulli's equation explain the reason for the drop in pressure at the stenotic tube.

The Bernoulli's equation is an energy conservation statement for flowing fluids. Thus, it is defined as:

energy per unit volume before = energy per unit volume after

$$P_1 + \frac{1}{2}pv_1^2 + pgh_1 = P_2 + \frac{1}{2}pv_2^2 + pgh_2$$

where P_1 is the pressure energy, $\frac{1}{2}pv_1^2$ is the kinetic energy per unit volume and pgh_1 is potential energy per unit volume.

Based on the velocity equation, the velocity is inversely proportionate to the surface area. It means when the fluid flows through a narrowed tube, the velocity will increase. By applying the Bernoulli's principle, the pressure of the fluid will decrease secondary to the high velocity to maintain the constant energy of the fluid.

Following this principle, the pressure of the CSF is expected to drop at the stenotic area as the velocity will increase. This drop in pressure is similar to the finding reported when the CSF flow rate increased, or stenotic size at Aqueduct increased (Hadzri *et al.*, 2011).